Journal of Biomedical Optics

SPIEDigitalLibrary.org/jbo

Real-time phase-contrast imaging of photothermal treatment of head and neck squamous cell carcinoma: an *in vitro* study of macrophages as a vector for the delivery of gold nanoshells

Taeseok Daniel Yang
Wonshik Choi
Tai Hyun Yoon
Kyoung Jin Lee
Jae-Seung Lee
Sang Hun Han
Min-Goo Lee
Hong Soon Yim
Kyung Min Choi
Min Woo Park

SPIE

Real-time phase-contrast imaging of photothermal treatment of head and neck squamous cell carcinoma: an *in vitro* study of macrophages as a vector for the delivery of gold nanoshells

Taeseok Daniel Yang,[a] Wonshik Choi,[a] Tai Hyun Yoon,[a] Kyoung Jin Lee,[a] Jae-Seung Lee,[b] Sang Hun Han,[b] Min-Goo Lee,[c] Hong Soon Yim,[c] Kyung Min Choi,[c] Min Woo Park,[d] Kwang-Yoon Jung,[d] and Seung-Kuk Baek[d]
[a]Korea University, Department of Physics, Seoul, Republic of Korea
[b]Korea University, Department of Materials Science and Engineering, Seoul, Republic of Korea
[c]Korea University, Department of Physiology, Seoul, Republic of Korea
[d]Korea University, Department of Otolaryngology-Head and Neck Surgery, Seoul, Republic of Korea

Abstract. Photothermal treatment (PTT) using nanoparticles has gained attention as a promising alternative therapy for malignant tumors. One strategy for increasing the selectivity of PTT is the use of macrophages as a cellular vector for delivering nanoparticles. The aim of the present study is to examine the use of macrophages as a cellular vector for efficient PTT and determine the appropriate irradiation power and time of a near-infrared (NIR) laser using real-time phase-contrast imaging. Thermally induced injury and death of cancer cells were found to begin at 44°C to 45°C, which was achieved using the PTT effect with gold nanoshells (NS) and irradiation with a NIR laser at a power of 2 W for 5 min. The peritoneal macrophage efficiently functioned as a cellular vector for the NS, and the cancer cells surrounding the NS-loaded macrophages selectively lost their cellular viability after being irradiated with the NIR laser. [DOI: 10.1117/1.JBO.17.12.128003]

Key words: real-time imaging; photothermal treatment; macrophage; gold nanoshells; squamous cell carcinoma.

Paper 12642 received Sep. 26, 2012; revised manuscript received Nov. 8, 2012; accepted for publication Nov. 21, 2012; published online Dec. 12, 2012.

1 Introduction

The primary treatments for head and neck cancers are surgery, radiation, chemotherapy, antibody-blocking therapy, or a combination of these methods. Although there have been advancements in the management of head and neck cancers to achieve cure with organ preservation, there has been little improvement in survival rates over the past 50 years, and the disease is still incurable.[1] The lack of improvement in survival rates may be due to the limitations of surgical resection of several adjacent important structures that are associated with functions such as speaking or swallowing, the high failure rate and toxicity of radiation therapy for advanced tumors, poor cell specificity and high toxicity of chemotherapy, and the limited supportive role of chemotherapy in concurrent chemoradiation therapy. To overcome these inherent limitations of conventional treatments, hyperthermia treatment has emerged as a promising alternative therapy for malignant tumor, in addition to gene therapy and immunotherapy, for treating malignant tumors.[2]

Hyperthermia, which is defined as an elevated body temperature of more than 40°C, has been used as an adjuvant therapy with chemotherapy and radiotherapy.[3] As cellular injury or death by hyperthermia at temperatures greater than 40°C results from protein denaturation,[4] the thermal treatment affects both healthy and cancerous tissues. Therefore, hyperthermia treatments must be specifically targeted to the tumor while producing considerably less heat in the surrounding tissue. Recently, photothermal treatment (PTT) using nanoparticles has gained attention as an alternative to hyperthermia treatment through the use of lasers for thermal treatment due to advancements in nanotechnology.

When nanosized metallic particles are stimulated by light, the conduction-band electrons on the surface of the particles exhibit surface plasmon resonance (SPR), and the energy of the irradiated light is lost through light scattering or light absorption. The absorbed light energy is converted into heat, which can be used for PTT. By changing the size, shape, structure, and composition of the nanoparticles, the peak frequency, the point at which nanoparticles scatter and absorb the maximum intensity of light, can be controlled over the visible or infrared spectrum.[5]

Nanoshells (NS) represent a new class of optically tunable nanoparticles consisting of a dielectric silica core and an ultrathin metallic coating layer (gold).[6,7] The relative core and shell thickness of a NS can be modulated to absorb light at near-infrared (NIR) wavelengths, which is a desirable optical window in human tissue for the deep penetration of light. The heat generated by the wavelength-specific resonance of the NS can be used to selectively kill malignant tumors that are susceptible to less heat than normal tissue, and this photothermal effect has been successfully tested using *in vitro* and *in vivo* models.[6–8] Additionally, the use of macrophages as cellular-based delivery vehicles for NS has been examined in several previous studies.[7,9,10]

Address all correspondence to: Seung-Kuk Baek, Korea University, Department of Otolaryngology-Head and Neck Surgery, Anam-dong 5-ga 126-1, Seongbuk-gu, Seoul 136-705, Republic of Korea. Tel: +(82)-2-920-5486; Fax: (82)-2-925-5233; E-mail: mdskbaek@gmail.com

0091-3286/2012/$25.00 © 2012 SPIE

Because the toxicity of nanoparticles is an important limitation for clinical applications, their use in humans requires further research and considerable caution.[11] Therefore, it is important to achieve the maximum PTT effect while using an appropriate power and time of laser irradiation with the lowest nanoparticle concentration possible. Additionally, it may be important to understand how the temperature near the nanoparticles increases due to NIR laser irradiation for certain power and irradiation times.

In most previous studies, examining cell destruction and death by PTT,[6,7,10] treatment effects were measured by evaluating the final stationary conditions using various staining methods to detect cell viability. However, cell death is not an instantaneous event but is rather a progressive phenomenon that results from continuous damage to the cell. Therefore, to determine the appropriate conditions for killing cells, real-time evaluations of the cell condition should be the first consideration. In particular, when considering the PTT hyperthermia effect, information about momentary changes in the cell status is necessary to determine the appropriate conditions for an effective PTT.

The objective of the present study is to determine the appropriate power and time of NIR laser irradiation by comparing the temperature required to kill cancer cells by heating with that induced by the photothermal effect at a specific NS concentration. Furthermore, this study examines momentary changes in cell status resulting from the thermal effect using real-time phase-contrast imaging and evaluates the use of macrophages as a cellular vector for delivering a sufficient quantity of NS to induce a sufficient photothermal effect for selectively killing cancer cells.

2 Materials and Methods

2.1 *Nanoshells*

Gold chloride trihydrate ($HAuCl_4 \cdot 3H_2O$, cat. no. 520918), ammonium hydroxide solution (30% NH_3 as NH_4OH assay, cat. no. 221228), ethanol (cat. no. 459828), tetraethyl orthosilicate (TEOS, cat. no. 333859), sodium hydroxide (NaOH, cat. no. 306576), tetrakis (hydroxymethyl)phosphonium chloride solution (THPC, 80% aqueous solution, cat. no. 404861), (3-aminopropyl)trimethoxysilane (APTMS, cat. no. 281778), potassium carbonate (cat. no. 367877), and formaldehyde solution (cat. no. F8775) were purchased from Sigma-Aldrich (Milwaukee, Wisconsin). Ultrapure water from a Direct-Q3 system (18.2 $M\Omega \cdot cm$, Millipore, Billerica, Massachusetts) was used in this work. A Cary 5000 ultraviolet-visible-NIR (UV-vis-NIR) spectrophotometer was used to measure the extinction of the nanoparticles.

Firstly gold nanoparticles (AuNPs, 2 to 3 nm in diameter) were synthesized by injecting an aqueous solution of $HAuCl_4$ (2 mL, 27 mM) into a mixture of pure water (45 mL), NaOH (0.5 mL, 1 M), and THPC (prepared by adding 12 μL of an 80% THPC aqueous solution to 1 mL water) with stirring. A dark-brown gold nanoparticle solution was obtained in 5 min.

Then, the silica core-gold shell nanoparticles were synthesized following a reported method with a few modifications.[12] The synthesis began with the addition of an ammonium hydroxide solution (3.5 mL, 30% NH_3 as NH_4OH assay) to 50 mL ethanol. The mixture was stirred vigorously, and 1.5 mL TEOS was added dropwise. The color of the solution changed to an opaque white. After the color change, the solution was continuously stirred for 30 min. Silica nanoparticles were obtained after centrifuging at 4600 g for 15 min, and they were then redispersed in pure water. To amino-functionalize the surface of the silica nanoparticles, 16.87 μL APTMS was added to 50 mL silica nanoparticle solution with vigorous stirring. The solution was continuously stirred for 1 h. Amino-functionalized silica nanoparticles were obtained after centrifuging at 4600 g for 15 min and were then redispersed in pure water. Amino-functionalized silica nanoparticle solution (500 μL) was added to 5 mL gold nanoparticle solution. The mixture was shaken gently for 2 to 5 min, allowed to sit for 2 h, centrifuged at 5000 rpm for 15 min, and then redispersed in pure water. For the growth of the gold NS, a growth solution was prepared by dissolving 0.025 g potassium carbonate in 100 mL water and stirring for 10 min. Subsequently, 1.5 mL of a 27-mM $HAuCl_4$ solution was added to the growth solution. After the yellow growth solution became clear, 27 μL formaldehyde was injected into a mixture containing 4 mL growth solution and 200 μL AuNP-amino-silica nanoparticle solution. The solution color began to turn blue, indicating the formation of gold NS. The NS were then suspended in serum-free medium (8.25×10^{10} particles/mL, 137 pM).

2.2 *Preparation of Head and Neck Cancer Cells and Mouse Peritoneal Macrophages*

The SNU-1041 squamous cancer cell line derived from human pharyngeal cancer was cultured in 500 mL RPMI 1640 (Gibco BRL, Grand Island, New York) mixed with 50 mL fetal bovine serum (Gibco BRL) in a 5% CO_2 incubator. The peritoneal macrophages were prepared from ICR outbred mice (which were 6 to 8 weeks old and had been intraperitoneally injected with 10 mL PBS), after which they were isolated from the PBS cell suspension by adding a red blood cell (RBC) lysis buffer followed by centrifugation. The cultures were washed twice with RPMI 1640 to remove nonadherent cells after the peritoneal macrophages were allowed to adhere to the culture dish for 2 h. The macrophages were then collected using cell scrapers (SPL Life Sciences, Korea). These studies were performed under Animal Medical Center Institutional Review Board approval.

2.3 *Thermal Destruction of Cancer Cells*

Cell culture dishes containing only the cancer cell line without NS or NS-loaded macrophages were mounted on an indium tin oxide (ITO) heating plate and placed in a live cell chamber at 37°C with 5% CO_2. The live cell chamber was mounted onto the sample stage of an inverted microscope (IX71, Olympus) operating in phase-contrast mode. An objective lens (20×, NA 0.45) was used to deliver the image to the CCD camera (pco. 1600 s, Photon Lines, Banbury, Oxfordshire, United Kingdom), which has a pixel resolution of 0.5 μm/pixel. Time-lapsed images of the cancer cells were acquired at 5-s intervals for 1 h. A temperature probe (Fluke 51II digital thermometer, Fluke, Everett, Massachusetts) was used for real-time monitoring of the temperature of the ITO plate and the culture dish [Fig. 1(a)]. The heat destruction rate of the cancer cells was calculated from the relative fraction of the acellular area, which was derived from the heating-induced cellular destruction. The Image *J* software package (National Institutes of Health, Bethesda, Maryland) was used to analyze the images. In addition, a lactate dehydrogenase (LDH) cytotoxicity assay (CytoTox 96, Promega, Madison, Wisconsin) was used to confirm that the

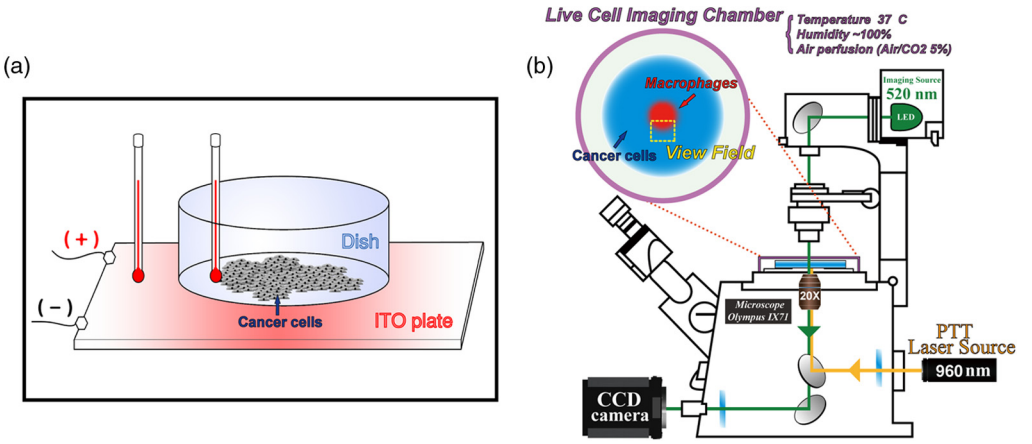

Fig. 1 Schematic diagram of thermal destruction and photothermal treatment (PTT) study using real-time phase-contrast imaging system with live cell chamber. The live cell imaging chamber is designed to maintain the temperature of culture medium at 37°C with saturated moisture and a fixed atmosphere of air/ CO_2. (a) The live cell imaging chamber with the cancer cell line on an indium tin oxide (ITO) heating plate is heated to calculate the heating-induced cellular destruction rate. (b) The light source for phase-contrast imaging is a 525-nm-wavelength LED, and the source for the PTT is a 960-nm-wavelength laser. A region containing both the cancer cell line (blue area) and the nanoshell-loaded macrophages (red area) is irradiated using a 960-nm-wavelength laser and estimated using real-time phase-contrast imaging system (dotted square).

cells had been destroyed by heating, since LDH is a stable cytosolic enzyme and is released from the cytoplasm by cellular lysis.

2.4 *Uptake of Nanoshells in Peritoneal Macrophages and Transmittance Measurement*

We loaded various concentrations of the NS suspension (10, 20, 50, 100, 200, 400, and 600 μL from 8.25×10^{10}/mL, 1.37 to 82.2 pM) into the peritoneal macrophages. The NS suspension was co-incubated with 2 mL peritoneal macrophages (1×10^4/mL) by shaking gently in a 15-mL tube for 1 h. The mixture containing the NS and macrophages was seeded into a 35-mm cell culture dish, incubated for 2 h to allow the cells to settle and adhere to the bottom, and rinsed three times using Hanks' balanced salt solution with calcium chloride and magnesium chloride (HBSS, Gibco, Carlsbad, California) to remove the NS that were not ingested by the macrophages. The NS-loaded macrophages adhered to the bottom were collected with cell scrapers. Finally, we made the cell suspension with 1×10^4/ml of the NS-loaded macrophages.

Additionally, the approximate uptake of NS by the peritoneal macrophages was estimated by measuring the reduced light transmission as a function of NS concentration. The reduction in transmission was expected to be quite small because of the low concentration of NS within the macrophages; thus, we reduced the intensity of the NIR laser to the lowest level that the camera (pco. 1600 s) could detect with a 10-s exposure time.

2.5 *Preparation of the Cancer Cell Monolayer Model*

The macrophages loaded with NS were forced to adhere to the center of the cell culture dish. Then, the SNU-1041 squamous cancer cell line (1×10^5/2 mL) was spread onto the dish and incubated overnight to allow the macrophages and cancer cells sufficient time to interact.

2.6 *Photothermal Treatment and Phase-Contrast Imaging*

The cell culture dish containing the cancer cell line and macrophages was placed in a live cell chamber at 37°C temperature with 5% CO_2. Time-lapsed images of a prepared specimen were acquired at 5-s intervals, typically for a time period of 1 h.

A region containing both cancer cells and NS-loaded macrophages was illuminated using a NIR laser (IPG Photonics, Oxford, Massachusetts) with a wavelength of 960 nm at irradiances ranging from 2 to 5 W/cm^2 with a laser spot size of 600 μm [Fig. 1(b)].

3 Results

3.1 *Characterization of Silica Core–Gold Shell NS*

Silica core–gold shell NS were synthesized following a reported method with a few modifications.[12] The synthesis begins with the preparation of monodispersed spherical silica nanoparticles using the method of Stöber et al.[13] The surface of the silica particles is further amino-functionalized to carry a positive charge, which is used to attract the negatively charged gold seeds. The gradual growth of the gold NS was observed over a period of 1 h with a distinctive color change to blue caused by the SPR of the gold NS. The silica core–gold shell nanoparticles were analyzed by transmission electron microscopy (TEM) and were observed to have a silica core (157 nm in diameter) that was evenly coated with a thin gold NS (14 nm thick) [Fig. 2(a)]. The optical properties of the silica core–gold shell nanoparticles were analyzed by measuring their UV-vis-NIR spectrum. An extinction maximum was obtained at 960 nm (λ_{MAX}) [Fig. 2(b)]. Considering that silica core–gold shell nanoparticles with a core diameter of 100 nm and a shell thickness of 30 nm exhibit an extinction maximum at 728 nm (λ_{MAX}),[14] the red shift of the λ_{MAX} observed in our work is reasonable because of the increased core:shell ratio.

3.2 *Thermal Destruction of Cancer Cells*

The cancer cells heated on the ITO heating plate were shrunk and detached from the bottom of the dish when the temperature increased in the culture dish. The relative fraction of the cellular area began to decrease after approximately 20 min of heating, and the temperature of the culture media was 44°C to 45°C when this process began [Fig. 3(a) and 3(b)]. The LDH cytotoxicity

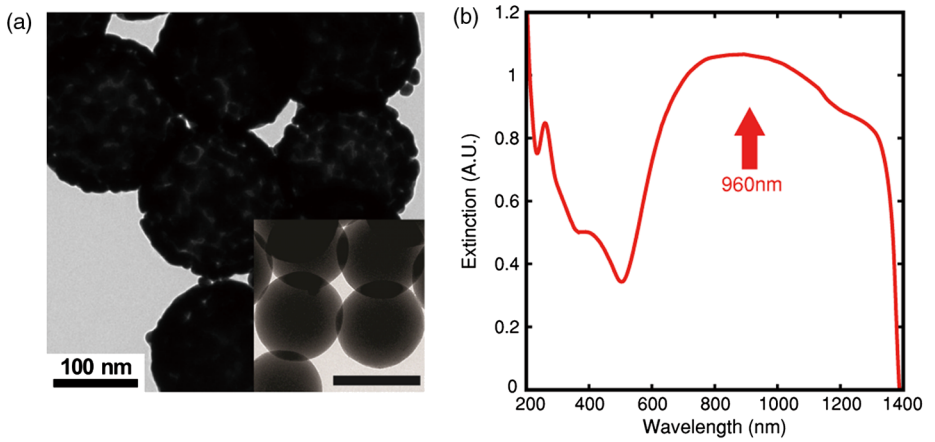

Fig. 2 Electron microscopy imaging and optical properties of the nanoshell. (a) Transmission electron microscopy (TEM) image of the nanoshells and uncoated silica particles (inset). Scale bar in the inset = 160 nm. (b) Ultraviolet-visible-near infrared (UV-vis-NIR) spectrum of the nanoshells. An extinction maximum (λ_{MAX}) is obtained at 960 nm.

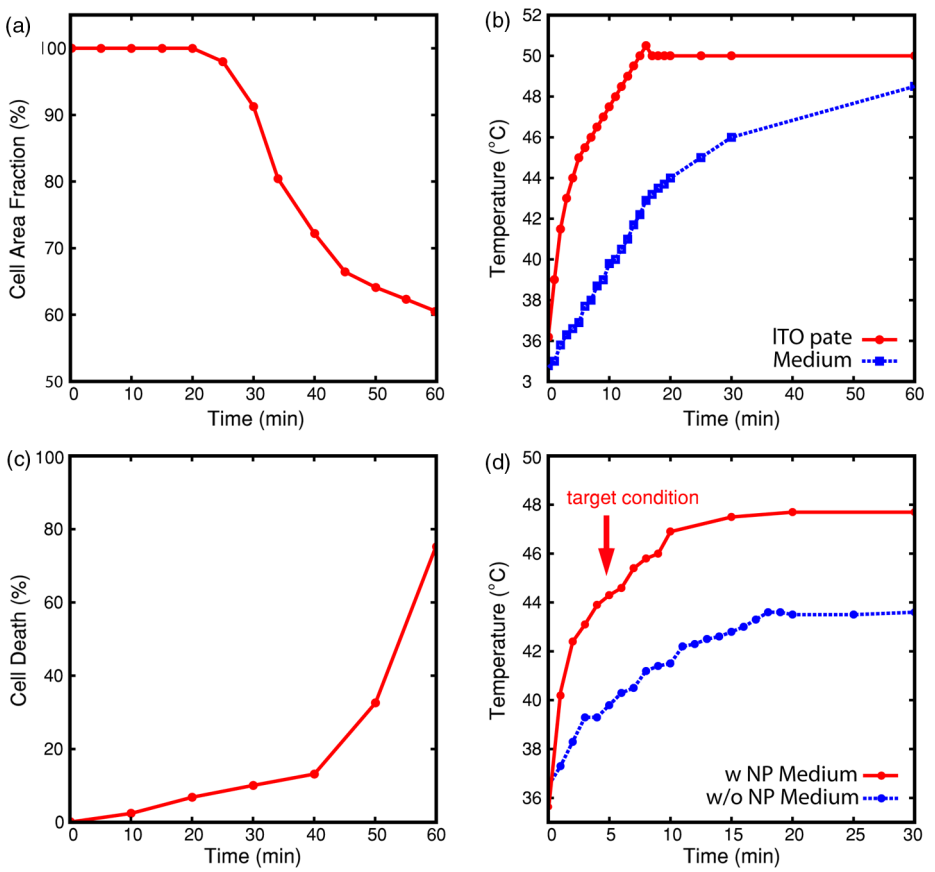

Fig. 3 Cancer cell viability with respect to increasing temperature from ITO plate heating and laser irradiation. Each plot shows a single time-course measurement. (a) Relative change in the living cell area with heating time (the area at $t = 0$ is normalized to 100%). An abrupt change in the cell area occurs at approximately 20 min. (b) Temperatures measured at the ITO heating plate and within the culture dish as a function of time. At 20 min, the temperature of the culture medium adjacent to cancer cells is >44°C (Video 1) (c) Cell death rate measured using the lactate dehydrogenase (LDH) assay during heating. The LDH level rises with increasing heating time. (d) Temperature change induced by irradiation with an NIR laser (2 W/cm^2). The culture medium is continuously illuminated with an NIR laser for 30 min, and the nanoshell (NS)-mixed medium contains only NS at a concentration of 27.4 pM. The red dots with a solid line represent the measured temperature in the NS-mixed medium during irradiation, and the blue dots with a dashed line represent the measured temperature in the medium without NS during irradiation. The red arrow indicates the treatment time required to reach the target temperature (5 min, 44°C to 45°C) (Video 1, MOV, QuickTime, 4.3 MB) [URL: http://dx.doi.org/10.1117/1.JBO.17.12.128003.1].

assay, which was used to validate that the cell area fraction is a good indicator of the cell death, demonstrated that heat induced the death of the cancer cells [Fig. 3(c)]. We confirmed that the increase in the LDH level and the decrease in the cellular area fraction were in good agreement, although there was a slight time lag between the two processes.

We investigated the effect of pure NS on the heating of the medium. The culture dish containing only NS (27.4 pM) in the culture media was irradiated using 960-nm laser light at an irradiance of 2 W/cm^2 and a laser spot size of 600 μm in diameter. When a temperature probe was used to measure the temperature change in the culture media of the central area within the laser beam, it was found that the heating effect by PTT with an irradiance of 2 W/cm^2 for 5 min achieved a temperature of 44°C to 45°C, the same temperature observed for the thermal cell destruction study [Fig. 3(d)]. However, the temperature of the culture dish without NS did not increase to the cell destruction temperature, even when the laser irradiation was continuously maintained.

Additionally, the NS-mixed media with various concentrations of NS were illuminated with NIR laser to evaluate the photothermal effect according to NS concentration within culture media. The target condition, in which the temperature of the culture media is >44°C with an irradiance of 2 W/cm^2 for 5 min, was achieved with a NS concentration of 1.37 pM or more. However, at a NS concentration of <1.37 pM, the temperature of the culture media was not significantly increased [Fig. 4(a)].

When the thermal destruction of cancer cells by ITO plate heating and the effect of pure NS on the heating of the medium were evaluated repeatedly, the results of each time-course measurement were reproducible.

3.3 *Macrophage Endocytosis of Gold NS*

To quantify the NS that were phagocytized by the peritoneal macrophages, we examined the relative change in transmittance with respect to the concentration of NS that were co-incubated with the macrophages, because macrophages containing more NS have a lower transmittance.

The relative transmittance of NS by peritoneal macrophages decreased with increasing NS co-incubation concentration [Fig. 4(b)]. Although the number of NS loaded into the peritoneal macrophages can be increased by using higher concentrations of NS, the cellular functions of the macrophages, such as migration, may be impacted. Because the safe concentration of NS for macrophages is lower than the saturation concentration at which macrophages can no longer phagocytize NS, we determined that the optimal co-incubation NS concentration was 27.4 pM.

We compared macrophages with and without NS using quantitative phase imaging and differential interference contrast imaging [Fig. 5(a) and 5(b)] and observed that small aggregates of NS were dispersed throughout the cellular cytoplasm of the NS-loaded macrophages.

3.4 *Effects of Photothermal Treatment with the NS-Loaded Macrophages*

The two monolayer models of squamous cancer cells, with or without the NS-loaded macrophages, were exposed to 960-nm NIR irradiation with increasing power from 2 to 5 W.

The monolayer model without the NS-loaded macrophages exhibited no changes in cellular viability after PTT [Fig. 5(c)]. However, in the monolayer model containing the NS-loaded macrophages, the cancer cells surrounding the NS-loaded macrophages decreased in size and detached from the bottom of the culture dish, indicating a loss in cellular viability [Fig. 5(d)]. Although the cellular death rate increased significantly with increasing power and exposure time of the NIR laser, the photothermal effect killed only the cancer cells that were adjacent to the NS-loaded macrophages.

4 Discussion

The combination of surgery, radiotherapy, and chemotherapy is typically the preferred treatment for advanced-stage head and neck cancers. However, when residual or reoccurring tumors remain after the aforementioned combination of treatments, these conventional treatments cannot be repeatedly used because of their high failure rate and toxicity. Many alternative treatments, including gene therapy, immunotherapy,

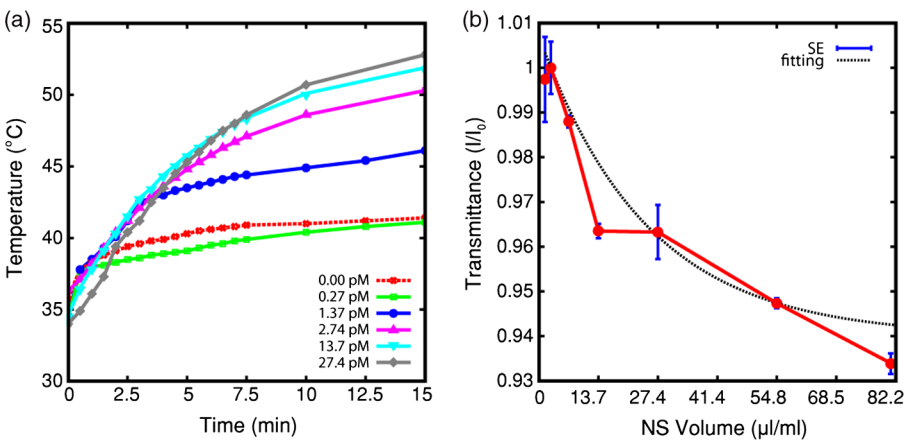

Fig. 4 Changes in the culture medium temperature and the macrophage endocytosis rate with respect to the NS concentration. (a) The medium temperature with changing NS concentration within the NS-mixed medium. The culture medium is continuously illuminated with an NIR laser for 30 min. The temperature of culture medium increases with increasing NS concentration, and the target temperature (>44°C to 45°C) is not achieved in low concentrations (<1.37 pM), irrespective of irradiation time. (b) Light transmittance of the NS-loaded macrophages. The light transmission decreases with increasing NS concentration that is co-incubated with the macrophages.

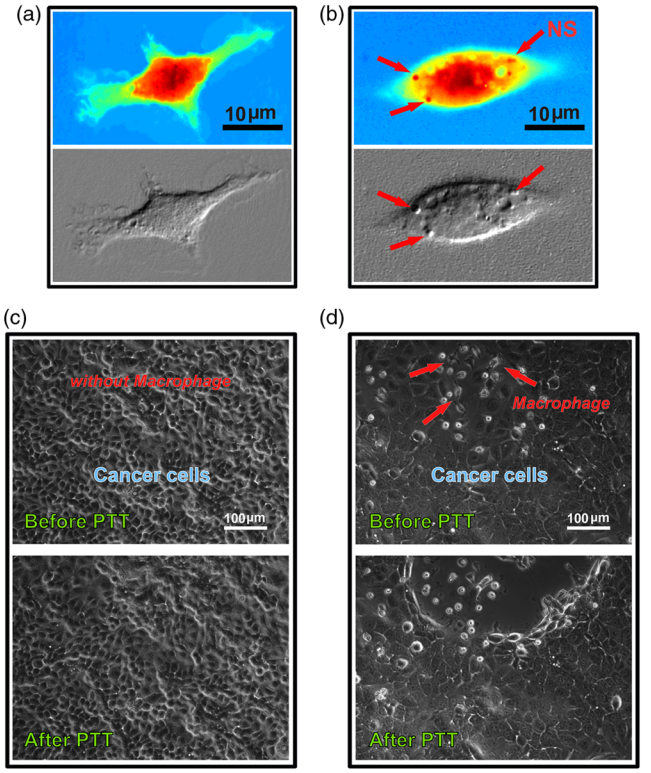

Fig. 5 Photothermal treatment using NS-loaded macrophages. (a) Quantitative phase image (top) and differential interference contrast image (bottom) of a macrophage without NS. (b) Quantitative phase image (top) and differential interference contrast image (bottom) of a macrophage with small NS aggregates (red arrows). (c) Phase-contrast image of cancer cells without macrophages before (top) and after (bottom) 5 min of laser irradiation at 2 W (control). (d) Phase-contrast image of cancer cells with the NS-loaded macrophages before (top) and after (bottom) 5 min of laser irradiation. This image shows selective cell death near the NS-loaded macrophages (Video 2, MOV, QuickTime, 4.2 MB) [URL: http://dx.doi.org/10.1117/1.JBO.17.12.128003.2].

hyperthermia, and photodynamic/photothermal therapy, have been studied to overcome the limitations of conventional therapies and demonstrate their efficacy as a targeted cancer therapy with cancer specificity.[2–5,15]

PTT is a field of photonics that uses nanotechnology to reduce the negative effects of existing hyperthermia and photodynamic treatments and to achieve specificity for cancer cells. However, because it is difficult to predict the toxicity of nanoparticles *in vivo*, PTT using nanoparticles should be performed with a lower concentration of nanoparticles and a lower laser power for a shorter time to prevent injury to the healthy tissue. Therefore, it is important to find the optimal conditions for an effective and safe PTT. In addition, antibody-conjugated nanoparticles with specificity for surface antigens of the tumor or macrophages with phagocytized nanoparticles have been used in previous studies to acquire specificity for tumors.[7,9,10,16]

The first goal of the present study was to determine the temperature and time required to kill cancer cells by heating. Furthermore, the appropriate nanoparticle concentration and the minimum illumination time needed for a particular NIR laser power to achieve the final temperature were also examined. Cell death occurs from the gradual accumulation of intracellular damage when cells are continuously exposed to heat. Therefore, to determine these subtle conditions, we performed real-time phase-contrast imaging to identify momentary changes in cell status during heating or PTT. The second aim of the study was to demonstrate that mouse peritoneal macrophages can phagocytize nanoparticles and that the PTT effect occurring near the macrophages loaded with nanoparticles can sufficiently kill cancer cells under the conditions determined in the first phase of the study.

In the present study, the cancer cells heated on the ITO heating plate began to be killed when the temperature of the culture dish was 44°C to 45°C and the heating effect by PTT with an irradiance of 2 W/cm^2 for 5 min achieved the same temperature.

Although many previous studies have reported the photothermal effect of nanoparticles, the most challenging problem is measuring the local temperature at the surface of the nanoparticles. Previous studies have investigated the threshold temperature at which cancer cells are destroyed.[6,17] Although the irradiation conditions, such as the wavelength and power of the laser and the irradiation time, were different, the threshold temperature observed in the previous studies was 70°C to 80°C, which is much higher than our result. This discrepancy in the thermal destruction temperature may result from the different methods used to estimate the temperature. Huang et al.[17] estimated the threshold temperature using numerical calculations of the local temperature rise in PTT and demonstrated the thermal destruction of cancer cells at 70°C to 80°C by heating in an oven using a cell culture model. The thermal death of cells was evaluated using trypan blue stain. Although the numerically calculated temperature agreed with the results of the oven heating study, the real temperature required to destroy cancer cells in culture media may be lower because the destruction of cells caused by a continuous temperature rise may be more effective than abruptly heating in an oven. Furthermore, it is difficult to estimate the real-time changes in the cells resulting from heating by using trypan blue staining, because the staining method can detect only the stationary and final status of cellular condition. In our study, because the cancer cells in the culture media were continuously heated using an ITO heating plate and the destruction of the cells was monitored using time-lapsed images at 5-s intervals for 1 h, the thermal destruction of cells may be detected earlier and the estimated threshold temperature may be lower. However, other studies have reported that the photothermal effect on a single gold nanoparticle in liquid increases the temperature by approximately 10°C to 20°C, which is similar to our result and is in good agreement with the target temperature estimated from the ITO heating plate.[18,19] Furthermore, 44°C to 45°C is sufficient for thermally induced cell injury and death.[20]

Previous studies have reported that the photothermal effect on cell death increases with increasing nanoparticle concentration and/or output laser power. In this study, the photothermal effect had a tendency to increase as a function of the NS concentration at 1.37 pM or more, and the target temperature (greater than 44°C to 45°C) was not achieved in concentrations lower than 1.37 pM. This result may mean that the least NS concentration at PTT target region should be 1.37 pM or more and it is possible to achieve the sufficient photothermal effect even at the considerably lower NS concentration used in contrast with previous studies, which employed micromolar nanoparticle concentrations.[19,21]

The primary functions of macrophages are to engulf and digest foreign materials. The ability of macrophages to phagocytize several types of nanoparticles, including gold NS, has

been reported in several previous studies.[7,9,10] When NS are uptaken by macrophages, they have a tendency to aggregate within the macrophage vacuoles.[7] Therefore, PEGylated NS, which exhibit less aggregation than bare NS, may be more suitable for achieving the photothermal effect by NIR laser light. In addition, due to the biocompatibility of gold, the NS were found to be nontoxic to the macrophages.

In the present study, the PEGylated gold NS phagocytized by peritoneal macrophages increased as a function of the co-incubation NS concentration, and the small aggregates of NS were observed throughout the cytoplasm of the macrophages, preserving their cellular viability at the co-incubation NS concentration of 27.4 pM. Furthermore, the NS-loaded macrophages showed enough selective photothermal effect to kill the cancer cells around them with an irradiance of 2 W/cm^2 for 5 min.

Peripheral blood monocytes have a natural ability to accumulate in and around tumor masses by a chemo-attractive gradient. When monocytes traverse the endothelial basement membrane, they differentiate into macrophages and then infiltrate a tumor. Such macrophages are referred to as tumor-associated macrophages (TAMs). Previous studies have reported that TAMs promote tumor progression, and the presence of large numbers of TAMs is associated with poor prognosis in various malignancies.[22] This outcome may be related with the nature of TAMs: the hypoxic and necrotic regions within tumors into which TAMs are recruited are associated with radiotherapy or chemotherapy resistance and with sources of subsequent local recurrence and distant metastasis.

Therefore, the target region of PTT should be these hypoxic regions. However, the efficacy of nanoparticle-based therapies that exploit the enhanced permeability and retention (EPR) effect or nanoparticles with antibodies or peptides specific to malignant cells may be limited due to the lack of tumor vasculature within such hypoxic or necrotic regions.

In other words, considering that infiltration of macrophages correlates with tumor hypoxia and necrosis,[23] macrophages may be useful as a cellular-based vehicle to deliver nanoparticles into hypoxic regions within the tumor mass, and then the photothermal effect from the nanoparticles delivered by the macrophages may effectively destroy the TAMs and the surrounding tumor cells. Additionally, although controlling the quantity of nanoparticles phagocytized by the macrophages may be difficult, macrophage-based delivery of nanoparticles has the advantage of preventing the uncontrollable spreading of nanoparticles that may result from the leaky nature of intratumoral vessels and of maintaining a specific concentration of nanoparticles within a target region. However, although it is questionable whether the injected macrophages may promote tumor progression and bad prognosis like TAMs, thorough study about macrophage toxicity should precede the clinical application of macrophages for PTT.

In conclusion, although many studies have examined PTT using nanoparticles, most have described the treatment effects by evaluating the final stationary condition using various staining methods. The present study suggests that the real-time monitoring of cell conditions using phase-contrast microscopy may be very important for understanding the cell death rates achieved and may provide a more accurate estimation of the PTT effect. In addition, macrophages can be useful as a cell-based vector to deliver nanoparticles into tumors, and the nanoparticles phagocytized by macrophages can selectively kill only the neighboring cancer cells through the plasmonic photothermal effect of an NIR laser.

The present assessment of the PTT effect was performed *in vitro*. We believe that our results will serve as an important basis for future studies of PTT application *in vivo*. Because the lack of NIR-absorbing chromophores in most biological tissues permits the transmission of light at NIR wavelengths, including 960 nm, normal tissue should receive minimal damage and NIR lasers may be a useful tool for clinical applications.

Although the toxicity of nanoparticles and macrophages is an important limitation for clinical applications, the use of cellular vectors such as macrophages may reduce the uncontrollable spreading and toxicity of nanoparticles and should enable more selective PTT for cancer cells. Additionally, it may be possible to deliver the nanoparticles effectively into the hypoxic and necrotic regions within the tumor mass.

Acknowledgments

This study was supported by Grant-in-Aids for Korea University Research and Business Foundation and Scientific Research from the Communication Disorders Center, Korea University.

References

1. J. A. Bonner et al., "Radiotherapy plus cetuximab for squamous-cell carcinoma of the head and neck," *N. Engl. J. Med.* **354**(6), 567–578 (2006).
2. A. V. Ambade et al., "Effect of suicide gene therapy in combination with immunotherapy on antitumour immune response and tumour regression in a xenograft mouse model for head & neck squamous cell carcinoma," *Indian J. Med. Res.* **132**, 415–422 (2010).
3. A. M. Westermann et al., "First results of triple-modality treatment combining radiotherapy, chemotherapy, and hyperthermia for the treatment of patients with stage IIB, III, and IVA cervical carcinoma," *Cancer* **104**(4), 763–770 (2005).
4. X. He et al., "*In situ* thermal denaturation of proteins in dunning AT-1 prostate cancer cells: implication for hyperthermic cell injury," *Ann. Biomed. Eng.* **32**(10), 1384–1398 (2004).
5. I. H. El-Sayed, "Nanotechnology in head and neck cancer: the race is on," *Curr. Oncol. Rep.* **12**(2), 121–128 (2010).
6. L. R. Hirsch et al., "Nanoshell-mediated near-infrared thermal therapy of tumors under magnetic resonance guidance," *Proc. Natl. Acad. Sci. U. S. A.* **100**(23), 13549–13554 (2003).
7. S. K. Baek et al., "Photothermal treatment of glioma; an *in vitro* study of macrophage-mediated delivery of gold nanoshells," *J. Neurooncol.* **104**(2), 439–448 (2011).
8. J. A. Schwartz et al., "Feasibility study of particle-assisted laser ablation of brain tumors in orthotopic canine model," *Cancer Res.* **69**(4), 1659–1667 (2009).
9. J. C. Kah et al., "Critical parameters in the pegylation of gold nanoshells for biomedical applications: an *in vitro* macrophage study," *J. Drug Target.* **17**(3), 181–193 (2009).
10. M. R. Choi et al., "A cellular Trojan Horse for delivery of therapeutic nanoparticles into tumors," *Nano Lett.* **7**(12), 3759–3765 (2007).
11. C. Medina et al., "Nanoparticles: pharmacological and toxicological significance," *Br. J. Pharmacol.* **150**(5), 552–558 (2007).
12. T. Pham et al., "Preparation and characterization of gold nanoshells coated with self-assembled monolayers," *Langmuir* **18**(12), 4915–4920 (2002).
13. W. Stöber et al., "Controlled growth of monodisperse silica spheres in the micron size range," *J. Colloid Interface Sci.* **26**(1), 62–69 (1968).
14. S. J. Oldenburg et al., "Nanoengineering of optical resonances," *Chem. Phys. Lett.* **288**(2–4), 243–247 (1998).
15. R. Ge et al., "An *in vitro* and *in vivo* study of combination therapy with Photogem®-mediated photodynamic therapy and cisplatin on mouse cancer cells (CT-26)," *Photomed. Laser Surg.* **29**(3), 155–160 (2011).

16. I. H. El-Sayed et al., "Selective laser photothermal therapy of epithelial carcinoma using anti-EGFR antibody conjugated gold nanoparticles," *Cancer Lett.* **239**(1), 129–135 (2006).
17. X. Huang et al., "Determination of the minimum temperature required for selective photothermal destruction of cancer cells with the use of immunotargeted gold nanoparticles," *Photochem. Photobiol.* **82**(2), 412–417 (2006).
18. M. Honda et al., "Nanoscale heating of laser irradiated single gold nanoparticles in liquid," *Opt. Express* **19**(13), 12375–12383 (2011).
19. G. S. Terentyuk et al., "Laser-induced tissue hyperthermia mediated by gold nanoparticles: toward cancer phototherapy," *J. Biomed. Opt.* **14**(2), 021016 (2009).
20. J. R. Lepock, "Cellular effects of hyperthermia: relevance to the minimum dose for thermal damage," *Int. J. Hyperthermia* **19**(3), 252–266 (2003).
21. Y. Li et al., "Copper sulfide nanoparticles for photothermal ablation of tumor cells," *Nanomedicine (Lond.)* **5**(8), 1161–1171 (2010).
22. R. D. Leek et al., "Association of macrophage infiltration with angiogenesis and prognosis in invasive breast carcinoma," *Cancer Res.* **56**(20), 4625–4629 (1996).
23. R. D. Leek et al., "Necrosis correlates with high vascular density and focal macrophage infiltration in invasive carcinoma of the breast," *Br. J. Cancer* **79**(5–6), 991–995 (1999).